Evaluation of the aerosol indirect effect in marine stratocumulus clouds: Droplet number, size, liquid water path, and radiative impact

Cynthia H. Twohy,[1] Markus D. Petters,[2] Jefferson R. Snider,[2] Bjorn Stevens,[3] William Tahnk,[1] Melanie Wetzel,[4] Lynn Russell,[5] and Frédéric Burnet[6]

Received 9 June 2004; revised 24 September 2004; accepted 10 February 2005; published 20 April 2005.

[1] Data from nine stratocumulus clouds in the northeastern Pacific Ocean were analyzed to determine the effect of aerosol particles on cloud microphysical and radiative properties. Seven nighttime and two daytime cases were included. The number concentration of below-cloud aerosol particles (>0.10 μm diameter) was highly correlated with cloud droplet number concentration. Droplet number concentrations were typically about 75% of particle number concentration in the range of particle concentrations studied ($\leq$400 cm^{-3}). Particle number was anticorrelated with droplet size and with liquid water content in drizzle-sized drops. Radiative impact also depends upon cloud liquid water content and geometric thickness. Although most variability in these macroscopic properties of the clouds could be attributed to variability in the large-scale environment, a weak anticorrelation between particle concentration and cloud geometric thickness was observed. Because of these variations, no correlation between calculated cloud optical thickness or albedo and particle concentration was detectable for the data set as a whole. For regions with comparable liquid water contents in an individual cloud, higher particle concentrations did correspond to increased cloud optical thickness. These results verify that higher particle concentrations do directly affect the microphysics of stratiform clouds. However, the constant liquid water path assumption usually invoked in the Twomey aerosol indirect effect may not be valid.

Citation: Twohy, C. H., M. D. Petters, J. R. Snider, B. Stevens, W. Tahnk, M. Wetzel, L. Russell, and F. Burnet (2005), Evaluation of the aerosol indirect effect in marine stratocumulus clouds: Droplet number, size, liquid water path, and radiative impact, *J. Geophys. Res.*, *110*, D08203, doi:10.1029/2004JD005116.

1. Introduction

[2] Theoretical and observational studies indicate that the properties of clouds are sensitive to the concentration, size and chemical characteristics of the ambient aerosol, since aerosol particles may act as cloud condensation nuclei (CCN). *Twomey* [1974] recognized the connection between increasing aerosol particle number concentration, decreasing droplet size, and increasing cloud reflectance. This effect thus has been termed the Twomey aerosol indirect effect, in contrast to the direct radiative effect of aerosols in clear air.

[3] Local enhancements to the atmospheric aerosol through the injections of particles associated with ship exhaust have been associated with "tracks" in clouds, i.e., linear regions of locally higher aerosol particle and cloud droplet concentrations and greater cloud reflectivities [*Radke et al.*, 1989; *Durkee et al.*, 2000]. Effects of urban aerosol particles on clouds have also been noted [e.g., *Fitzgerald and Spyers-Duran*, 1973; *Barrett et al.*, 1979], and positive relationships between aerosol particle number and droplet number have been compiled [*Leaitch et al.*, 1992; *Martin et al.*, 1994]. Most recently, analyses of field measurements made during the second Aerosol Characterization Experiment (ACE-2 [*Brenguier et al.*, 2000a; *Guibert et al.*, 2003; *Snider et al.*, 2003]) and the Cirrus Regional Study of Tropical Anvils and Cirrus Layers–Florida Area Cirrus Experiment (CRYSTAL-FACE) [*VanReken et al.*, 2003; *Conant et al.*, 2004] demonstrated the utility of comprehensive studies based on multi-instrument and multiplatform investigations. In ACE-2, it was demonstrated that cloud optical thickness varies, as expected, like $N^{1/3}$ (N being the droplet concentration), when variations of cloud geometric thickness are taken into account [*Brenguier et al.*, 2000b].

[4] Satellite measurements have shown that urban pollution causes a shift to smaller droplet sizes in locations far removed from the source of the pollution [*Kim and Cess*, 1993; *Han et al.*, 1994; *Twohy et al.*, 1995; *Wetzel and Stowe*, 1999]. Although most research into aerosol effects

[1]College of Oceanic and Atmospheric Sciences, Oregon State University, Corvallis, Oregon, USA.
[2]Department of Atmospheric Sciences, University of Wyoming, Laramie, Wyoming, USA.
[3]Department of Atmospheric Sciences, University of California, Los Angeles, California, USA.
[4]Desert Research Institute, Reno, Nevada, USA.
[5]Scripps Institution of Oceanography, University of California, San Diego, La Jolla, California, USA.
[6]Meteo-France, Centre National de Recherches Météorologiques, Météorologie Expérimentale et Instrumentale, MNP, Toulouse, France.

0148-0227/05/2004JD005116$09.00

on clouds has focused on low-lying stratiform clouds, some investigators have noted possible aerosol effects on cirrus [e.g., *Sassen et al.*, 1995; *Ström and Ohlsson*, 1998]. Pollution from urban areas may also decrease precipitation, since too many small droplets deplete available water vapor so that precipitation-sized drops cannot form [*Albrecht*, 1989; *Rosenfeld*, 2000]. These changes in cloud albedo and lifetime may counteract the greenhouse effect and could have dramatic impacts on global climate change [*Charlson et al.*, 1992]. However, direct observation of expected effects of aerosol particles on cloud visible reflectance have been elusive, possibly due to variations in liquid water path [e.g., *Twohy et al.*, 1995; *Han et al.*, 2002; *Brenguier et al.*, 2003].

[5] *Charlson et al.* [1987] noted that clouds most affected by the Twomey indirect effect should be those with visible albedos near 0.5, similar to albedos of marine stratiform clouds over the oceans. *Twomey* [1991] and *Platnick and Twomey* [1994] show that cloud albedo susceptibility, or the sensitivity of albedo to changes in droplet number concentration, is inversely proportional to droplet number concentration. Thus radiative properties of marine stratiform clouds with relatively low droplet concentrations are those which should be most influenced by additional aerosol particles that act as CCN. While satellite measurements are extremely valuable in determining radiative properties over large regions, in situ measurements are needed to reliably determine properties of the aerosol, which may induce changes in radiative properties. In this study, we present microphysical measurements of aerosol particles and stratiform clouds off the California coast. In a future manuscript, we will present chemical properties of the same aerosol particles and clouds.

2. Experiment

[6] This research was part of the Dynamics and Chemistry of Marine Stratocumulus-II (DYCOMS-II) experiment, an airborne field program conducted during July of 2001 [*Stevens et al.*, 2003]. The C-130 aircraft operated by the National Center for Atmospheric Research (NCAR) was used to measure stratocumulus clouds over the eastern Pacific Ocean, off the coast of San Diego, California. DYCOMS-II sought to better understand the microphysics and dynamics of marine stratocumulus clouds, with an emphasis on nocturnal characteristics that have been largely unmeasured in the past. A well-mixed boundary layer covered by a dense, relatively uniform stratocumulus layer was encountered in nearly all of the nine flights, two of which were conducted during daytime. Many of the clouds were characterized by frequent drizzle [*Van Zanten et al.*, 2005], some with rates as high as several mm per day. Cloud-top entrainment velocities ranged from about 0.3 to 0.7 m s^{-1} [*Faloona et al.*, 2005].

[7] Each research flight began with a ferry to a region of horizontally homogeneous stratocumulus about 300 km offshore. For most flights, 60-km diameter circular patterns were conducted above cloud, below cloud-base, and near the ocean surface, as well as at two levels within the cloud itself near cloud base and cloud top. These in-cloud flight levels were selected after conducting soundings through the cloud layer and judging where the aircraft could remain in cloud the entire time, but still be as close to cloud base (or top) as possible. This somewhat subjective method led to some variation in height of the actual sampling, relative to the cloud geometric thickness, from flight to flight. On the basis of Forward Scattering Spectrometer Probe (FSSP) data from soundings, the mean ratio of cloud-base leg height to cloud thickness for the data presented here was 0.22 (standard deviation 0.083), while this ratio for the cloud-top legs was 0.72 (standard deviation 0.16).

[8] An effort was made to sample a single air mass by flying circular patterns relative to the mean wind at a given level. In practice, the sampling ended up being only approximately Lagrangian because of both varying horizontal wind speeds among levels (shear, which is most evident at cloud top) and in-flight adjustments mandated by the need to stay out of restricted areas. Flight patterns provided the opportunity to measure aerosol properties at two levels below the cloud as well as above the cloud, and to sample for relatively long periods within the cloud itself. Two flights (flights 6 and 9) focusing on radar retrievals utilized shorter flight legs. Of the nine flights discussed here, two (flights 8 and 9) were conducted during daylight hours while the others were at night. Further details of flight patterns and characteristics are given in *Stevens et al.* [2003, electronic supplement].

[9] The C-130 measured state parameters and chemical species and also carried a wide range of spectrometers to measure aerosol particle and cloud drop sizes. The total aerosol particle number concentration larger than 0.013 μm diameter was measured with a TSI 3760 condensation nucleus counter. The aerosol particle size spectrum was recorded by a radial differential mobility analyzer (RDMA [*Russell et al.*, 1996]) and a wing-mounted Particle Measuring Systems Passive Cavity Aerosol Spectrometer Probe (PCASP-100), which sized from 0.008 to 0.128 μm and 0.10 to 3.0 μm diameter, respectively.

[10] Size distributions from the RDMA were assumed to represent dry particles, since the relative humidity in that instrument was approximately 35%. RDMA distributions were corrected for changes in temperature and pressure in the instrument. Due to low counts, data from three size bins were combined in the lower channels of the RDMA. Past studies usually have assumed that PCASP size distributions also represented dry particles, since inlet heaters and deceleration warm the sample airflow. However, there is some indication from the DYCOMS-II data that the effective PCASP relative humidity varies with ambient relative humidity and that drying of sampled particles is not necessarily complete. This effect, which will be detailed in a forthcoming study, will produce some uncertainty in the actual dry sizes of the lowest PCASP channels but is not expected to substantially impact the average total PCASP number concentrations used in this study. The first channel of the PCASP (spanning nominally 0.09 to 0.10 μm diameter) was noisy and was removed from the total PCASP concentration presented here. For the composite size spectrum presented later (RDMA/PCASP), the RDMA was utilized in the overlap region of the instruments. Integrated concentrations of the composite spectrum agreed well with the total CN concentration.

[11] Cloud droplet size distributions were measured primarily with an FSSP-100 optical scattering probe with Droplet Measurement Technologies' upgraded electronics,

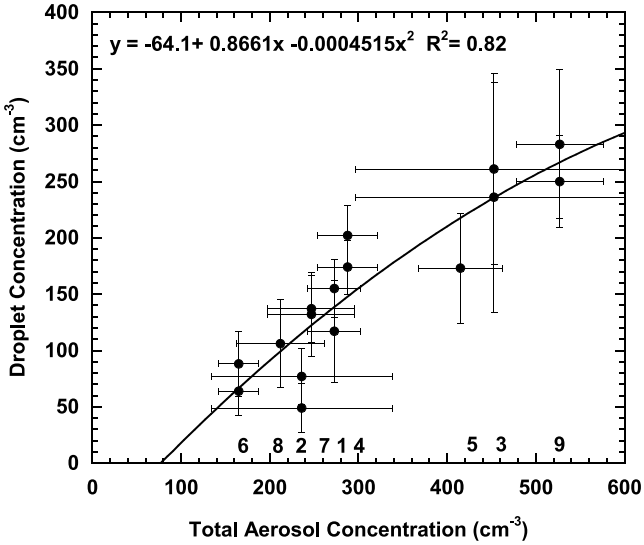

Figure 1. Mean below-cloud total aerosol particle concentration (>0.013 μm diameter) versus mean droplet concentration for all DYCOMS-II flights (FSSP-100 with SPP upgrade was used to measure droplet concentration for all flights except 5 and 6, when the Fast-FSSP was used). Cloud-base and cloud-top droplet concentrations were similar, but both are included for completeness. "Error" bars represent one standard deviation from the mean of the 1 Hz data. Uncertainty in the CN number concentration is less than 10% [*Twohy*, 1991], and uncertainty in the FSSP number concentration is about 27% [*Baumgardner et al.*, 1990]. Flight numbers are given below the data points for reference. One cloud-base outlier from flight 5, with a very low liquid water content of only 0.07 g m^{-3}, was removed. Note that the polynomial curve fit shown here is only valid within the range of our measurements, from about 160 to 530 particles cm^{-3}.

but for two flights when FSSP-100 data were not available, the "Fast-FSSP" [*Brenguier et al.*, 1998] was used. Two hot-wire probes [*King et al.*, 1985] were used to measure liquid water in the cloud droplet size range (about 3 to 60 μm diameter). A 260-X and 2D-C optical array probe measured the large cloud drop to drizzle drop size range (size limits 25 to 635 μm and 42 to 1592 μm, respectively). These probes gave similar results for number concentration and liquid water content, although the 260-X sometimes exhibited electronic noise outside of cloud. Since drizzle can break up in inlets and artificially increase particle concentrations [*Weber et al.*, 1998], below-cloud data coinciding with 2D-C concentrations ≥ 1 L^{-1} were removed from particle concentrations presented here.

3. Results

[12] In this section, correlations between aerosol particle number concentration and various cloud properties are presented. Statistical significance for each relationship is assessed using a simple one-tailed t-test at a probability level of 0.05. If the t value for the observations, t_{obs}, is greater than the critical t value, t_{crit}, the correlation may be considered significant. In Table 1 of section 3.4, these statistical results are compiled for each of the cloud properties analyzed.

3.1. Droplet Number and Size

[13] Several previous studies have measured relationships between aerosol particle concentration and droplet concentration in various cloud types. While droplet concentration has generally been determined by single particle scattering spectrometers, different measures of aerosol particle concentration have been employed. These include total particle number as measured by condensation nucleus (CN) counters [e.g., *McFarquhar and Heymsfield*, 2001], larger particle number as measured by single particle scattering spectrometers [e.g., *Martin et al.*, 1994; *Gultepe et al.*, 1996], and even cloudwater sulfate mass [*Leaitch et al.*, 1992]. The ACE-2 study led to the conclusion that calculations based on aerosol property measurements can overpredict measured CCN and cloud droplet concentrations, especially in polluted air masses.

[14] Figure 1 shows the correlation between mean below-cloud total particle concentration (from the CN counter) and mean in-cloud droplet concentration for all nine flights in

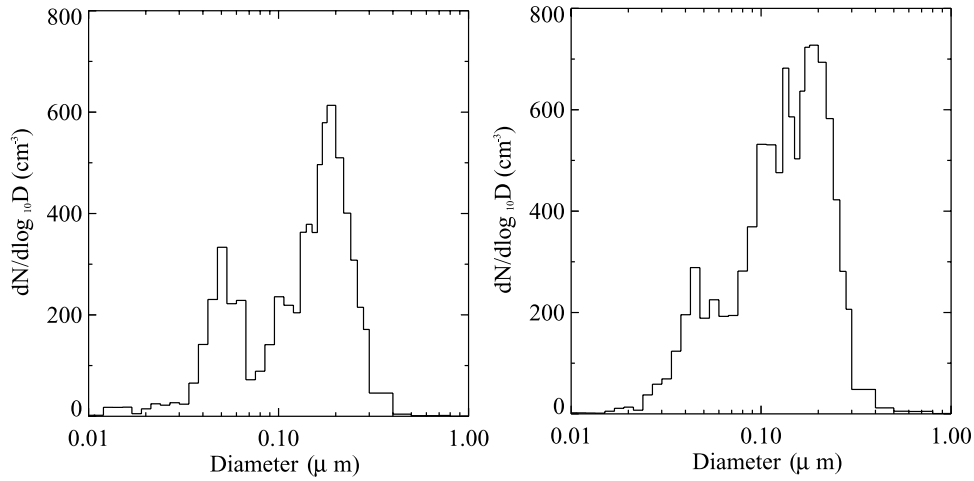

Figure 2. Below-cloud particle size distribution measured from the RDMA and PCASP combined for flight 8 (left) and flight 3 (right).

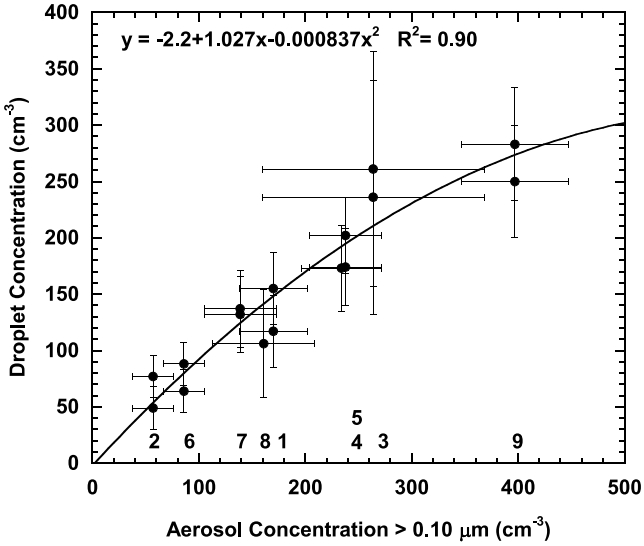

Figure 3. Same as in Figure 1, but using PCASP aerosol particle concentration (excluding the first channel) on the abscissa. Note that the polynomial curve fit shown here is only valid within the range of our measurements, from about 60 to 400 particles cm^{-3}.

the DYCOMS-II research area. For each data point, one Hz data were averaged over a 10 to 60 min leg of level flight. Both cloud-base and cloud-top measurements of droplet concentration are included for each flight, although values were similar and no consistent offset between cloud base and cloud top concentration was observed. This consistency of droplet concentration with height is typical for stratocumulus layers [*Noonkester*, 1984], while droplet size and liquid water content (LWC) increase with height [*Brenguier et al.*, 2000b]. The plot demonstrates that a strong and significant correlation (t_{obs} = 7.7, t_{crit} = 1.8) exists between below-cloud particle concentration and droplet concentration in these stratocumulus clouds.

[15] Detailed below-cloud particle size distributions that include the smallest particles measured by the RDMA usually exhibited a minimum in the size distribution at about 0.08 μm dry diameter (Figure 2). Data are shown on the left from flight 8, which was a daytime flight and on the right from flight 3, a nocturnal flight. This minimum was located well below the overlapping size region of the RDMA and PCASP, and was not usually observed in the above-cloud spectra; thus it is a real feature of the below-cloud size distributions. This feature has been observed by others and is thought to be caused by aqueous-phase chemistry, which can increase the size of residual nuclei remaining after evaporation of droplets from nonprecipitating clouds [*Hoppel et al.*, 1994]. Small particles, which have higher critical supersaturations and are less likely to nucleate, do not acquire additional mass; thus a size differential develops between the two populations over time. Near marine stratocumulus on the Washington coast, *Vong and Covert* [1998] found the Hoppel minimum to occur between 0.09 and 0.10 μm (dry diameter), while off the Oregon coast, *Frick and Hoppel* [1993] observed minima in particle distributions at about 0.12 μm (dry diameter).

[16] The scatter in Figure 1 is reduced and r^2 increases from 0.82 to 0.90 if only the larger particles measured by the PCASP (>0.10 μm diameter) are regressed with droplet number (Figure 3). The correlation for this size range is very significant (t_{obs} = 10.8, t_{crit} = 1.8) and suggests that these larger particles from below cloud not only have a dominant role in nucleation, but are the most important determinant of mean cloud droplet concentration in marine stratocumulus in this region. Particles larger than 0.10 μm account for about 90% of the particles above the minimum in the complete size distributions shown in Figure 2.

[17] *Heintzenberg et al.* [2000] reviewed global characteristics of marine aerosols and found mean particle concentrations over the 30°–45° northern latitude oceans to be about 460 cm^{-3}. 250 cm^{-3} of these, on average, were in the accumulation mode, as approximated by our PCASP concentration. Inspection of Figure 3 reveals that particle concentrations on flights 2, 6, 7, 8, and 1 were relatively low for the marine environment, on flights 4, 5, and 3 they were near average, and on flight 9 concentrations were substantially above average. Recognizing that much of the global marine boundary layer is subject to anthropogenic pollution [*Heintzenberg et al.*, 2000], relative descriptions of "clean," "intermediate," and "polluted" are given to the flights in the three groups specified above. Flights 8 and 9, the two daytime flights, fall in clean and polluted regimes, respectively. Back-trajectories for all flights were primarily

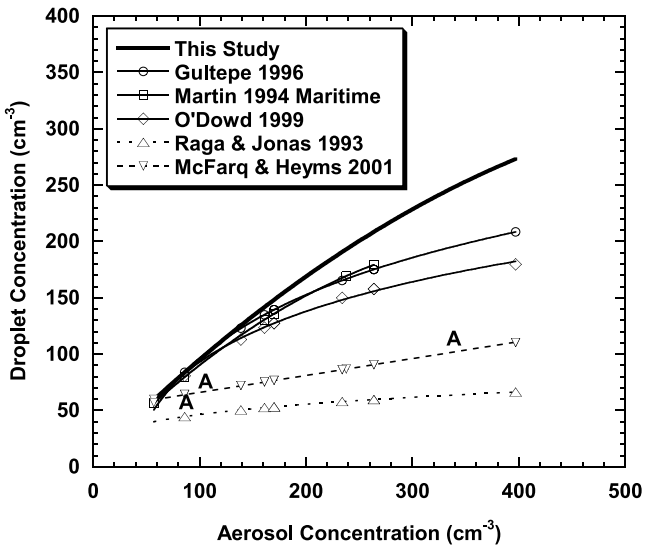

Figure 4. As in Figure 3, but with a polynomial fit to the DYCOMS-II data and parameterizations developed from other data sets included. All clouds were sampled over the ocean, but exhibited varying amounts of continental influence. Those with solid lines pertain to stratiform clouds [*Gultepe et al.*, 1996; *Martin et al.*, 1994; *O'Dowd et al.*, 1999; this study], while those with dotted lines are for small cumuli [*Raga and Jonas*, 1993; *McFarquhar and Heymsfield*, 2001]. Points marked with an "A" are values from the ACE-2 field experiment [*Brenguier et al.*, 2003]. All studies used accumulation-mode concentrations except McFarquhar and Heymsfield, who used total (CN) aerosol particle concentrations.

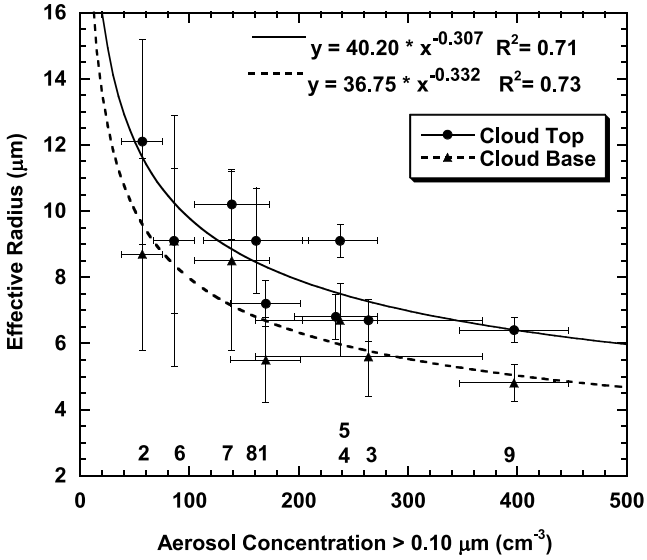

Figure 5. PCASP aerosol particle concentration versus drop effective radius at cloud top (circles) and cloud base (triangles). "Error" bars represent one standard deviation from the mean of the 1 Hz data. Note that the curve fit shown here is only valid from about 60 to 400 particles cm^{-3}.

northwesterly, yet particles can be transported all the way to the west coast of the United States from Asia [*Jaffe et al.*, 1999]. Single-particle electron microscopy revealed some black carbon, nonvolatile organics, and soil dust in some of the DYCOMS-II samples (in addition to the more prevalent sea-salt and sulfates). These measurements will be detailed in a later paper.

[18] In Figure 4, our results for mean particle concentration versus mean droplet concentration for DYCOMS-II are compared with maritime cloud data from other parts of the world. Our results are similar in magnitude with those of *Gultepe et al.*'s [1996], *Martin et al.*'s [1994], and *O'Dowd et al.*'s [1999] maritime data sets. Nearly all data sets show evidence of "roll-off" at higher aerosol concentrations, where cloud supersaturations are suppressed and a smaller proportion of potential CCN are activated [e.g., *O'Dowd et al.*, 1999; *Twohy et al.*, 2001]. The roll-off at higher concentrations has also been observed using satellite data and is expected to limit changes in shortwave radiative forcing by aerosols [*Wetzel and Stowe*, 1999].

[19] Data from the three studies discussed above were taken in stratiform clouds with relatively low aerosol particle concentrations, while the other two parameterizations in Figure 4 are based primarily on cumulus clouds with greater continental influence and higher particle numbers. These curves are not expected to match the maritime stratocumulus, but are included to demonstrate that relationships between aerosol particle number and droplet number vary with cloud type and geographic location. Points marked with an "A" are derived from the ACE-2 data set [*Guibert et al.*, 2003] and correspond to flights with aerosol particle concentrations within our range of interest (<400 cm^{-3}). These data were taken from stratocumulus in the northeast Atlantic and the most polluted of these cases plots substantially below the curves represented by the other maritime stratocumulus data sets. This departure is attributed partly to the systematically lower vertical velocity variability noted for the ACE-2 clouds [*Guibert et al.*, 2003] relative to the DYCOMS-II clouds. In support of this assertion we note that vertical velocity standard deviations measured in cloud during the seven nocturnal DYCOMS-II flights (flights 1 to 7) were on average 46% larger than an average of values reported by *Guibert et al.* [2003] (all daytime flights). Our explanation, however, cannot fully explain the discrepancy, as the DYCOMS-II flights 8 and 9 were daytime flights characterized by vertical velocity standard deviations comparable to those documented by Guibert et al. and these daytime points are not displaced as far below the DYCOMS-II line as is the polluted ACE-2 point. Whether or not aerosol shape effects [*Snider et al.*, 2003] or size-dependent vapor condensation kinetics [*Feingold and Chuang*, 2002] are responsible for this discrepancy remains an open issue.

[20] The Twomey indirect effect assumes that the vertically integrated LWC, or liquid water path (LWP), does not vary with increasing CCN. Under this assumption, increasing droplet number would result in a smaller average droplet size. In Figure 5, aerosol particle concentration is plotted against droplet effective radius r_e, the radiatively important parameter of the droplet size distribution [*Hansen and Travis*, 1974]. r_e was calculated using both the FSSP and 260-X probe, since the larger drops may contribute to this parameter in high-drizzle cases. For our data set, r_e was about 14% larger (on average) than the mean radius calculated from the FSSP alone.

[21] Figure 5 shows that the expected anticorrelation of aerosol particle number with droplet size holds for DYCOMS-II clouds. In this figure, cloud top and cloud base samples were regressed separately, since droplets at cloud base are smaller than those at cloud top. Taking this into account, the correlation is significant for both cloud regions (t_{obs} = 4.1, t_{crit} = 1.9 for cloud top; t_{obs} = 4.0, t_{crit} = 1.9 for cloud base). The $-1/3$ dependence is expected from simple calculations and has been discussed by others [*Vong and Covert*, 1998; *Brenguier et al.*, 2003]. Droplets in the cleanest case are almost twice as large as those in the most polluted case. However, the standard deviations of droplet sizes in the clean cases are larger than can be explained by the size increase alone, with the cleanest case having r_e standard deviations five to eight times as large as those in the more polluted case.

3.2. Drizzle

[22] Droplets need to grow larger than a threshold size to coalesce and form drizzle. Thus increasing aerosol particle concentration has been predicted to reduce cloud drizzle and increase cloud lifetime, the often called "second" aerosol indirect effect. Below-cloud particle number concentration was compared with different drizzle mode indicators. These included the number concentrations and drizzle water contents from both the 2D-C (40–800 μm) probe and the 260-X (40–620 μm) probe. All four variables were anticorrelated with particle number concentration, particularly at cloud top. The relationship with the 2D-C liquid water content is shown in Figure 6a (cloud top and cloud base plotted independently) and in Figure 6b (cloud top and cloud base values averaged). If cloud top and cloud base values of drizzle LWC are averaged, the linear correlation is particularly significant (t_{obs} = 5.1, t_{crit} = 1.9). (It is important to

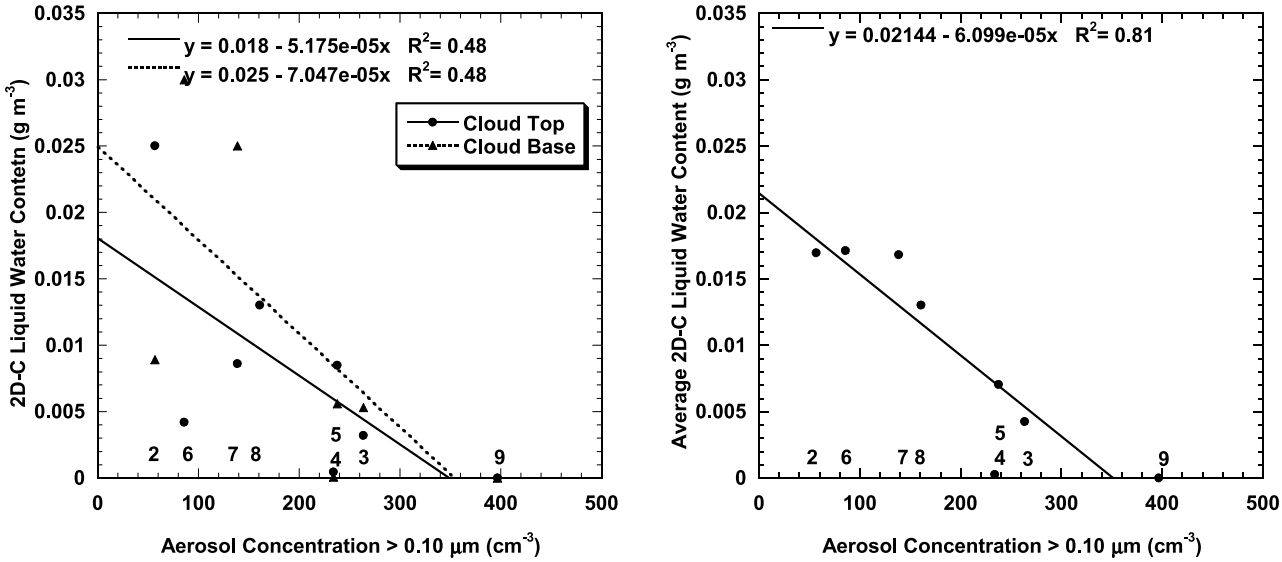

Figure 6. Aerosol particle concentration from the PCASP versus drizzle liquid water content integrated from the 2D-C imaging probe. Flight numbers are given below the data points for reference (2D-C data not available for flight 1). Standard deviations are not shown due to the large variance in the 2D-C data relative to mean values. (a) Data from cloud top and cloud base runs averaged individually. (b) Cloud top and cloud base runs averaged together. Note that the curve fit shown here is only valid from about 60 to 400 particles cm^{-3}.

note, however, that drizzle is inhomogeneous both vertically and horizontally, and so such relationships apply only in an average sense and not necessarily within discrete regions of the cloud layer.) The cleanest flights (2, 6, 7, and 8) have the largest drizzle LWCs (2D-C data from flight 1 were not available).

[23] *Yum and Hudson* [2002] observed anticorrelations between CCN number and drizzle in marine stratocumulus. They determined that drizzle is much more prevalent in clouds having mean droplet diameters larger than 15 μm, a size equivalent to an effective radius of about 8.5 μm. This approximately matches our results (compare Figure 5 with Figure 6b). The onset of precipitation is sensitive to the size of the biggest droplets in a cloud layer (precipitation embryos). The precipitation rate also depends on the available droplet liquid water content to be collected by the drizzle drops, which in turn depends on the cloud geometric thickness. This has been demonstrated by *Pawlowska and Brenguier* [2003] with the ACE-2 data set and *Van Zanten et al.* [2005] with the DYCOMS-II data set, both showing that the drizzle rate scales linearly with power laws of the cloud geometric thickness and droplet concentration.

[24] Drizzle itself can reduce aerosol particle concentrations through precipitation scavenging, which would tend to strengthen the negative correlations observed here and maintain low accumulation-mode particle concentrations. Very clean environments can also allow the nucleation of new small particles in cloud-free regions. This apparently occurred during flight 2 and is discussed by *Petters* [2004].

3.3. Radiative Impact

[25] In order for the Twomey effect to have climatic impact, pollution needs to influence not only the droplet size distribution, but also cloud optical thickness and albedo. These latter quantities are dependent on both effective radius and liquid water path. During ACE-2, the expected relationships between droplet concentration and cloud optical thickness were verified at the scale of the cloud cells [*Schüller et al.*, 2003], but when averaged at the large scale, variations of the cloud geometric thickness, or liquid water path, counterbalanced this trend and prevented remote sensing detection of the aerosol indirect effect [*Brenguier et al.*, 2003].

[26] Using satellite data and focusing on high aerosol particle concentrations, *Nakajima et al.* [2001] deduced a positive correlation between inferred aerosol number and cloud optical thickness. However, their Figure 4, which relates liquid water path and optical thickness to aerosol particle concentration, showed an inflection point at particle column concentrations of $10^{7.8}$ cm^{-2}. Below this point, liquid water path actually decreased with increasing particle concentration, and optical thickness was approximately constant. If we assume most of the particle number is confined within the boundary layer depth of about 1000 m, this inflection point corresponds to a particle number concentration of over 600 cm^{-3}. Hence, at lower particle concentrations, Nakajima et al.'s data apparently do not show Twomey's indirect effect on optical thickness. Satellite estimates of aerosol particle number are subject to large errors (up to a factor of 10 in absolute magnitude), so the actual value of this inflection point is highly uncertain until verified with in situ measurements.

[27] Since all our data are for relatively low aerosol particle concentrations, they provide an excellent opportunity to determine the dependence of optical properties on particle concentration in this lower aerosol regime. This is especially important since changes in droplet concentration with changes in aerosol particle concentration are greater at lower particle concentrations (see nonlinear slope of

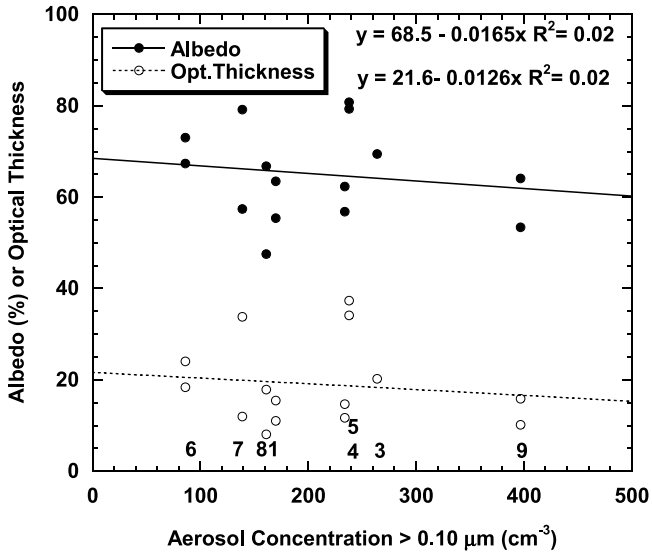

Figure 7. Aerosol particle concentration versus calculated cloud optical thickness and albedo (%) determined from two soundings for each flight, except #2. Horizontal error bars are omitted for clarity. Note that the curve fit shown here is only valid from about 60 to 400 particles cm^{-3}.

Figure 3). As discussed earlier, the susceptibility, or the change in albedo relative to the change in droplet number concentration, is potentially large in this regime [*Platnick and Twomey*, 1994].

[28] Cloud optical thickness, τ^*, can be approximated as follows, where ρ_w is the density of water and r_e is the effective radius [*Stephens*, 1978]:

$$\tau^* \approx (3\mathrm{LWP})/(2\rho_w r_e). \quad (1)$$

[29] Thus liquid water path and effective radius have approximately equal and opposite potential impacts on optical thickness. Optical thickness was calculated for our data set using vertically integrated liquid water content and average effective radius using one-second data from individual aircraft soundings through the cloud layer. For each flight, two soundings nearest in time to the below-cloud flight circle were utilized (except for flight 3 when quality data from only one sounding were available). While some repeat soundings (particularly during the daytime flights 8 and 9) showed substantial variations in cloud height, most repeat soundings showed within-flight variations that were smaller than variations between flights (Figure A1). For example, variations in cloud geometric thickness for the two repeat soundings on nighttime flights ranged from 9 m to 90 m (67 m to 127 m for daytime), while cloud thickness for soundings from all flights ranged between 230 m and 470 m. Using data from both soundings for each flight gives some indication of variation in cloud features, but it should be noted that soundings were always done at the same side of the flight circle and so may not describe the mesoscale variability for the full width of the flight circle.

[30] Cloud-top albedo (or reflectance), A_c, was estimated using the Eddington approximation [*Meador and Weaver*, 1980]:

$$A_c = [0.75(1-g)\tau^*][(1+0.75(1-g)\tau^*]^{-1}. \quad (2)$$

Here g is the asymmetry factor, which is assumed to be 0.85. This approximation assumes negligible absorption due to soot (black carbon) or other compounds, a reasonable supposition for typical eastern Pacific stratocumulus clouds. This was demonstrated by *Twohy et al.* [1989] and can be verified again using our electron microscope analysis of 100 impacted below-cloud particles from each of flights 5, 7, and 8. Particles were identified as soot by their chain-aggregate morphology and lack of detectable X-ray signature. A soot particle diameter of 0.18 μm (average of measured length and width), a particle density of 1.2 g cm^{-3}, and measured particle number concentrations and cloud liquid water contents were used to calculate soot concentrations in ng soot g^{-1} cloud water. Values obtained were 0, 400, and 700 ng soot g^{-1} cloud water for flight 7, 8, and 5, respectively. The two higher values are still an order of magnitude lower than those used for calculations of the "semidirect" effect by *Ackerman et al.* [2000] to represent more polluted conditions in the Indian Ocean. Using radiative transfer calculations, *Twohy et al.* [1989] showed that the cloud-top albedo change for a soot concentration of 600 ng soot g^{-1} cloud water would only be 0.001 (absolute magnitude) for an optical thickness of 30 and effective radius of 10 μm (λ = 0.475 μm). To effect a more substantial albedo change of 0.03, 2×10^4 ng soot g^{-1} cloud water would be required, about 30 times higher than measured on flight 5. Soot concentrations were not measured for the most polluted flight in our data set, flight 9, but given that total particle concentrations were only about 25% higher than for flight 5 (Figure 1), soot concentrations 30 times higher are unrealistic for this data set.

[31] In Figure 7, calculated optical thickness and albedo are shown as a function of aerosol particle concentration for the DYCOMS-II data set. No significant correlation between aerosol particle concentration and either optical thickness or albedo is apparent (t_{obs} = 0.6, t_{crit} = 1.8 for optical thickness; t_{obs} = 0.5, t_{crit} = 1.8 for albedo). While a lack of a relationship does not absolutely prove one does not exist for a larger data set (section 3.4), both the low correlation coefficient and the lack of any positive correlation between aerosol particle concentration and cloud optical properties suggest that increasing particle number did not, in fact, increase the albedo of the DYCOMS-II clouds. Therefore variations in optical properties must have been dominated by variations in liquid water content and cloud geometric thickness. As shown by *Austin et al.* [1995], cloud optical thickness is expected to vary with the 5/3 power of cloud geometric thickness and only the 1/3 power of droplet number concentration. Thus relatively small changes in cloud geometric thickness can counteract large changes in droplet number caused by additional CCN. Geometric thickness, liquid water content and liquid water path are further discussed in Appendix A.

3.4. Discussion of Significance

[32] Throughout this work, we have developed relationships between aerosol particle concentration and various cloud parameters for the DYCOMS-II data set using simple correlations. Table 1 summarizes t-test results used to determine whether the null hypothesis (that there is no relationship between particle concentration and the parameter of interest) can or cannot be rejected at a probability

Table 1. Significance of Relationships Between Aerosol Particle Concentration (>0.10 μm Diameter) and Cloud Parameters

Parameter	r^{2a}	r^{b}	n^{c}	$t_{obs}{}^{d}$	$t_{crit}{}^{e}$	Reject?[f]
Droplet Number[g]	0.90	(+) 0.95	16	10.8	1.8	Yes
Cloud Top Eff. Radius[h]	0.71	(−) 0.84	9	4.1	1.9	Yes
Cloud Base Eff. Radius[h]	0.73	(−) 0.85	8	4.0	1.9	Yes
Ave. Drizzle LWC[i]	0.81	(−) 0.90	8	5.1	1.9	Yes
Cloud Top Cloud LWC[j]	0.09	(−) 0.30	9	0.8	1.9	No
Cloud Base Cloud LWC[j]	0.02	(−) 0.14	8	0.4	1.9	No
Cloud Geom. Thickness (no flight 2)[k]	0.24	(−) 0.49	15	2.0	1.8	Yes
Liquid Water Path (no flight 2)[l]	0.11	(−) 0.33	15	1.3	1.8	No
Optical Thickness (no flight 2)[m]	0.02	(−) 0.16	15	0.6	1.8	No
Albedo (no flight 2)[n]	0.02	(−) 0.13	15	0.5	1.8	No

[a]Pearson coefficient of determination from the appropriate figure/regression.
[b]Pearson coefficient of correlation. Also denotes sign of relationship (positive or negative).
[c]Number of samples. Assumed to include both cloud top and cloud base data for the first parameter, and data from both soundings for the last four. While these pairs of samples could be considered not to be independent, our rejection conclusion would not change if a single value for each flight were used, except for cloud geometric thickness.
[d]Observed t value, equal to $r((df)/(1 - r^2))^{0.5}$; df, degrees of freedom (n − 2 except for droplet number when it is n − 3 due to second-order fit).
[e]Critical t value at p = 0.05, from statistical tables.
[f]If $t_{obs} > t_{crit}$, null hypothesis may be rejected.
[g]Droplet number concentration from FSSP (Figure 3).
[h]Effective radius from the FSSP and 260-X (Figure 5).
[i]Liquid water content from the 2D-C (Figure 6b).
[j]Liquid water content from the King hot-wire probe plus 2D-C.
[k]Cloud geometric thickness using sounding data and FSSP concentration (Figure A2) without flight 2.
[l]Liquid water path using sounding data and sounding LWC (Figure A3d) without flight 2.
[m]Cloud optical thickness using equation (1) (Figure 7) without flight 2.
[n]Cloud-top albedo using equation (2) (Figure 7) without flight 2.

level of 0.05. If the null hypothesis can be rejected, the relationship is statistically robust. A nonrejection of the null hypothesis (Type II error) does not necessarily indicate that no relationship exists, simply that it cannot be proven with this data set.

[33] Table 1 shows that the relationships between aerosol particle number and droplet number (positive), cloud-top effective radius (negative), and drizzle LWC (negative) are statistically significant. Cloud geometric thickness and the related liquid water path (discussed in Appendix A) exhibit negative relationships with particle number, but the t-values are just above and just below, respectively, the critical t-values necessary to establish statistical significance. Part of the difficulty in establishing significance lies in the small sample size and in the large variation in these parameters apparently due to dynamical, rather than microphysical processes. This variation can be a factor of two or more for the same below-cloud particle concentration (compare variations at concentrations of 240 cm^{-3} in Figures A2 and A3). Cloud-top liquid water content, optical thickness, and albedo have observed t-values well below those necessary to establish statistical significance.

4. Case Studies

[34] Above we presented overall statistics from nine DYCOMS-II flights, and showed that many average cloud characteristics, in particular droplet number, size, and drizzle amount, were related to the number concentration of larger (>0.10 μm) aerosol particles below cloud. Covariance in these properties occurred not only between flights, but within flights as well. On flights 8 and 3, substantial variations in particle number concentration were observed as the aircraft flew along its circular track below cloud. These variations were mirrored in the droplet properties and in some cases, these patterns were retained over long time periods throughout the quasi-Lagrangian flights.

[35] Figure 8 depicts below-cloud particle concentration and various cloud parameters for the daytime flight 8, moving from the east side of the flight track (high particle concentrations) to the west side of the track (low concentrations) and back to the east. The diameter of the circle was about 60 km. Corresponding to the higher aerosol particle concentrations were higher droplet concentrations, smaller effective radii, and lower drizzle concentrations. Liquid water contents were highly variable, especially to the west, but had similar mean values on both sides of the track. Approximate doubling of aerosol particle concentration on the east side of the track resulted in the same approximate doubling of droplet concentration. Values on both sides of the track match well with those expected from the overall project statistics presented in Figure 3.

[36] Derived cloud products available from the Moderate Resolution Imaging Spectroradiometer (MODIS) satellite instrument include droplet effective radius and cloud optical thickness. The Terra satellite carrying this instrument passed over the DYCOMS-II region at 18:40 UTC, about four hours prior to when the C-130 collected the data shown in Figure 8. The location of the flight circle was advected back with the mean wind to match the approximate cloud location at the time of the MODIS overpass. MODIS data at this location are shown in Figure 9. Despite the difference in sampling times, the MODIS-derived effective radius (Figure 9a) shows some similarity to that measured by the aircraft, with largest values on the west side of the track where the droplet concentration is lowest. The magnitudes of the MODIS r_e values, however, are much higher than in situ values (14.5 for MODIS versus 7.6 in situ on east side of track; 16.1 for MODIS versus 10.6 in situ on west side of track). MODIS data represent cloud-top values, while the flight data from flight 8 were actually taken about 72% of

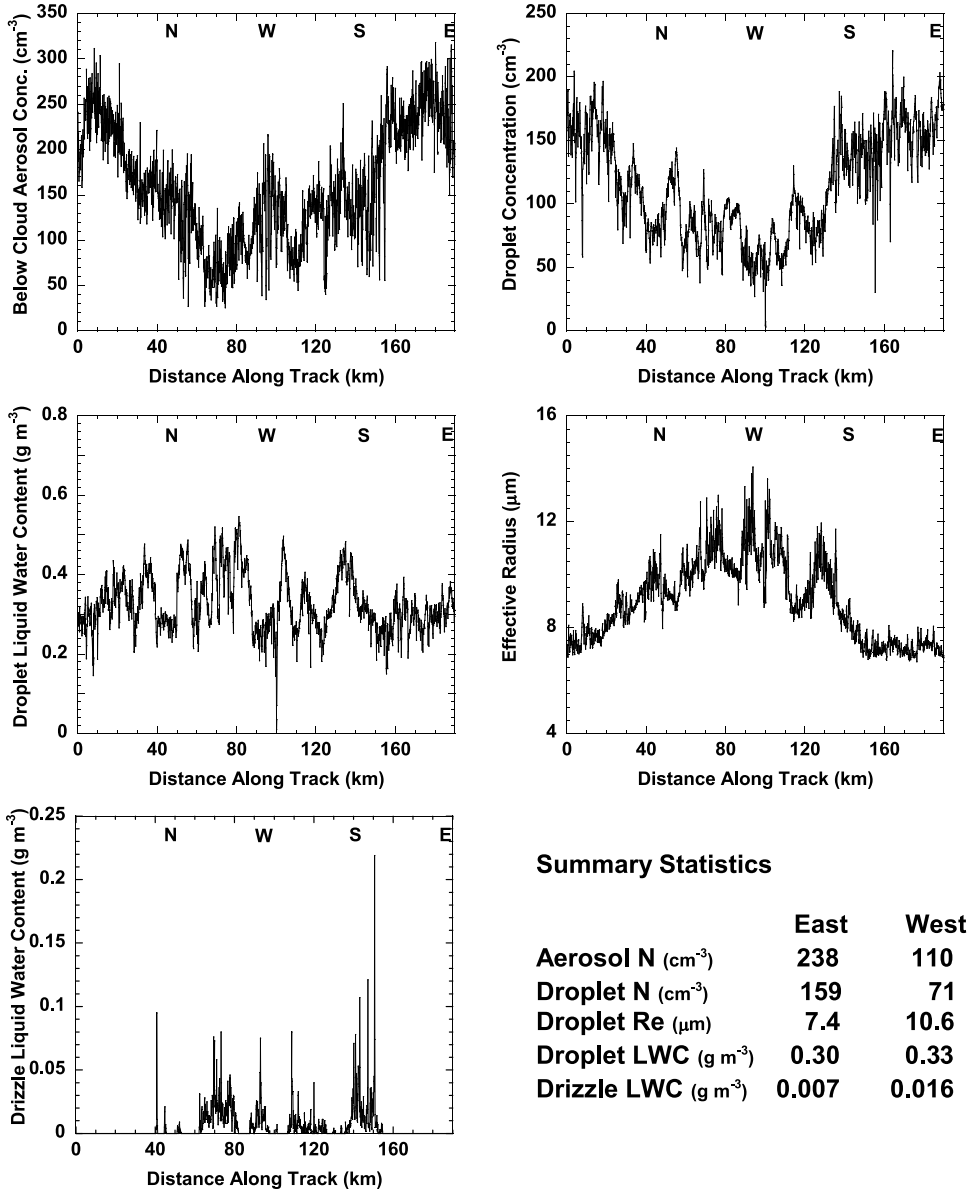

Figure 8. Relationship between aerosol particle concentration and various microphysical properties on flight 8 (daytime flight). Lower right pane gives mean values for partial legs approximately 36 km long at each side of the track.

the distance from cloud base to cloud top. On the basis of r_e profiles during soundings, this could explain 10–20% of the difference. Additionally, the MODIS overpass was in the morning, when the clouds tended to be thicker than in the afternoon when the aircraft was sampling. In fact, subsequent in situ sampling four hours later in the evening at about 20:00 local time (03:00 UTC) showed much higher liquid water contents, particularly on the west side of the track (although the circular variation in particle and droplet number, droplet size, and drizzle persisted). The MODIS optical thickness values (Figure 9b) show large variations that mimic the cellular structure of the liquid water, but are slightly higher overall on the east side of the track where the droplets are smaller ($\tau^*_{east} = 28.5$ versus $\tau^*_{west} = 24.2$).

[37] Cloud visible albedo can be derived from GOES satellite data, which were collected at 1 km resolution every 15 minutes during the DYCOMS-II project. GOES data were processed using SeaSpace TeraScan software, providing image pixel navigation, remapping, and calculation of albedo by scaling with solar zenith angle. Figure 10 shows GOES-10 albedo data for the cloud sampled in flight 8 with the aircraft flight track superimposed. While some high albedo values are present at the west side of the circle, they are more variable due to the pronounced cellular structure of the cleaner, drizzling clouds. Cloud albedo values were extracted from the satellite for the flight track location and are compared with droplet concentration and liquid water content in Figure 11. Albedo mimics the highly variable structure of the liquid water content, which exhibits large swings in the clean west part of the track. In order to directly test the Twomey effect, we selected segments of the cloud with similar liquid water contents, but with differing

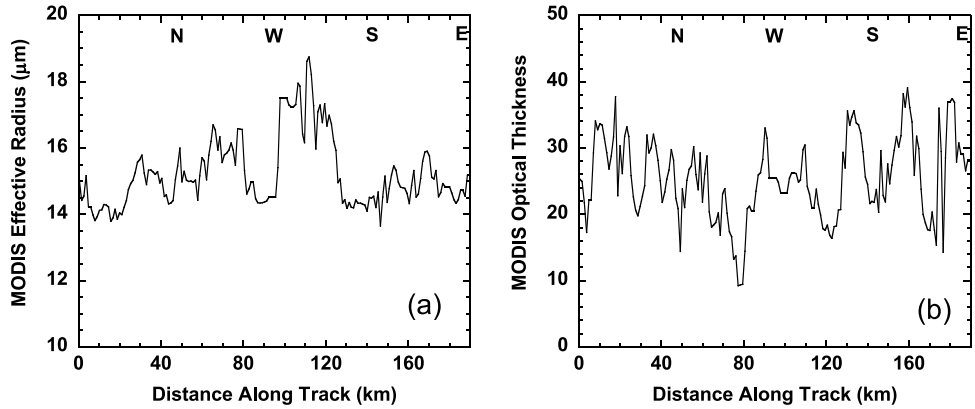

Figure 9. MODIS-derived (a) effective radius and (b) optical thickness measured four hours prior to the aircraft sampling of the cloud displayed in Figure 8.

droplet concentrations. These segments, the first with a mean LWC of 0.27 g m^{-3} and the second with a mean LWC of 0.28 g m^{-3}, are highlighted in Figures 11b and 11c. Segregating the data in this way allows the indirect effect to be clearly observed: an increase in droplet concentration by a factor of 2.8 leads to an albedo change from 0.325 to 0.458, an increase of about 40%.

[38] Aerosol particle concentrations were higher overall during flight 3, with a large variation in particle number observed between clouds on the south and north sides of the flight track (Figure 12). While aerosol particle number was closely related to droplet number for flight 3, a substantial increase in liquid water content on the north side of the track changed the droplet size and drizzle amounts from those expected by a simple interpretation of the indirect effect. Some drizzle was present throughout the track, yet mean droplet size and drizzle liquid water content were actually larger in the more polluted area with higher particle and droplet number concentrations. This demonstrates the important effect of dynamical processes. If one examines the south and north ends of the track independently, however, the expected anticorrelations of effective radius and drizzle amount with aerosol particle number can be seen. For example, on the south end of the track, the minimum in particle and droplet number corresponded with a maximum in droplet size and drizzle liquid water. The spike in particle and droplet concentration at about 40 km is a ship track that was clearly evident in the satellite imagery. In the ship track, while effective radius decreased slightly, no significant change in liquid water content was observed.

5. Summary and Conclusions

[39] DYCOMS-II stratocumulus clouds exhibited a strong relationship between below-cloud aerosol particle concentration and droplet microphysical properties. In particular, clouds forming in air with higher particle concentrations had higher droplet concentrations, smaller droplet sizes, and lower drizzle rates. The relationship between the number concentration of larger aerosol particles (>0.10 μm) and droplet number concentration was particularly strong, and seemed robust despite changes in diurnal cycle, liquid water content, and geometric cloud thickness. Overall, drizzle associated with low droplet concentrations did not cause substantial thinning of DYCOMS-II clouds.

[40] No relationship between aerosol particle concentration and either calculated cloud optical thickness or albedo was observed for the data set as a whole. These results imply that while the first part of the Twomey indirect effect, that higher aerosol particle concentrations lead to more, smaller droplets, is valid, the effect on cloud albedo may be obviated by concurrent changes in cloud thickness and liquid water path. In a case study where regions with similar liquid water contents were selected, however, satellite-

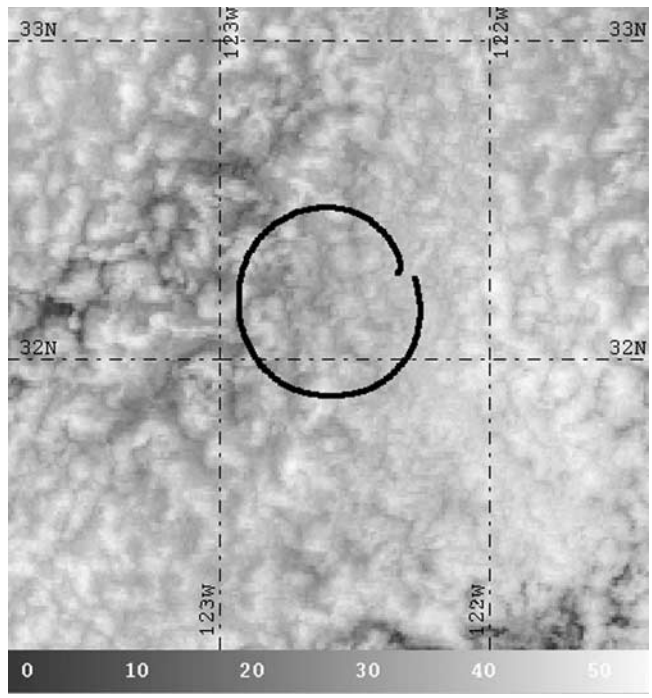

Figure 10. GOES visible albedo image taken during the sampling period of flight 8; the aircraft flight track is superimposed.

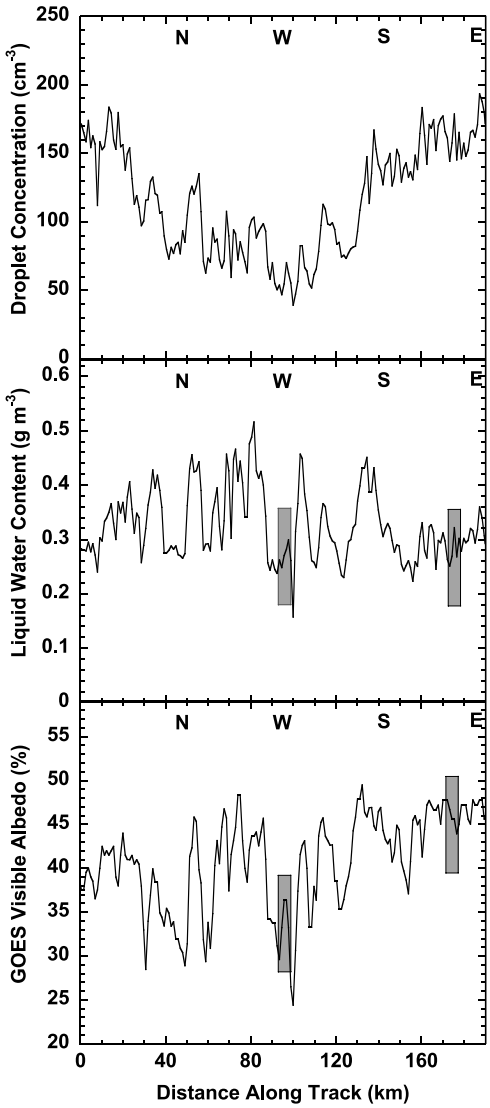

Figure 11. Droplet concentration, liquid water content, and visible albedo from GOES during the sampling period of flight 8. Region with similar LWCs discussed in the text is highlighted. Data have been averaged over a 10 s interval for clarity.

measured visible albedo was seen to increase in response to aerosol loading.

[41] Liquid water content and cloud thickness varied considerably for the nine DYCOMS-II flights, primarily due to dynamical influences. Both liquid water content and cloud thickness were weakly anticorrelated with aerosol particle concentration for the cloud data set as a whole. However, these relationships were barely significant at the 0.05 probability level for cloud thickness and not significant for liquid water path. The strong variation in cloud thickness and liquid water content due to dynamics means that these relationships would require a large data set to establish significance. More satellite studies are indicated, but will require in situ validation of aerosol and cloud properties.

[42] It is important to note that these results hold only for the eastern Pacific stratiform clouds sampled during DYCOMS-II. Further measurements are needed to determine effects on clouds in other regions, with different aerosol loadings and dynamic forcings. Also, the relationships developed here relate only to impacts of particle number concentration on cloud properties. The effectiveness of aerosol particles as CCN and their impact on cloud properties is expected to be dependent on particle size and chemical composition as well. These particle characteristics also elucidate source regions and therefore aid in understanding the degree of anthropogenic influence on cloud properties. DYCOMS-II aerosol and cloud chemical properties will be explored in future work.

Appendix A: Liquid Water Content, Geometric Thickness, and Liquid Water Path

[43] As discussed earlier, the first indirect effect invokes a constant liquid water path. On the other hand, some second indirect theories predict that drizzle will deplete cloud water content and aerosol to such an extent that the cloud layer will thin. As a consequence, radiative cooling at cloud-top would be reduced and the boundary layer is predicted to collapse [*Bougeaut*, 1985]. Additional aerosol particles may offset this effect and prolong cloud lifetime. The relationship between drizzle and cloud thermodynamics and structure, however, is complex. For example, drizzle has been predicted to actually strengthen convection and thicken clouds in some areas, while depleting them in others, generally increasing the variability in cloud properties [*Stevens et al.*, 1998]. The idea that precipitating stratocumulus cannot persist for long periods of time does not seem to be supported by DYCOMS-II clouds, some of which persisted for hours despite locally heavy drizzle rates [*Stevens et al.*, 2005].

[44] Studies of ship tracks, where aerosol particles from ships produce enhanced droplet number, have shown evidence that liquid water content/path may actually be related to aerosol particle concentration. With in situ measurements, *Radke et al.* [1989] found that liquid water content increased in ship tracks, apparently due to drizzle suppression; *Taylor et al.* [2000] found similar results for some, but not all ship tracks measured. On the other hand, *Coakley and Walsh* [2002] surveyed a large area with satellite data and concluded that liquid water path was usually lower in ship tracks than in surrounding clouds. *Ackerman et al.* [2004] postulates that LWP (and therefore the effectiveness of the indirect aerosol effect) is dependent upon the humidity of the air above the boundary layer. Liquid water content and cloud geometric thickness thus are critical variables to measure in the assessment of both indirect effects.

[45] Cloud optical thickness in an vertically stratified cloud increases as geometric thickness to the five-thirds power [*Brenguier et al.*, 2000b], and because of this sensitivity the comparison of clean and polluted clouds of slightly differing geometric thickness may not reveal a detectable Twomey indirect effect. In fact, there is empirical evidence that this may occur. *Twohy et al.* [1995] found that a polluted stratus cloud had a much higher droplet number concentration and smaller droplets than a clean cloud, but a change in visible albedo was not observed, indicative of a larger liquid water path in the clean case. *Han et al.* [2002] used satellite data to show that the liquid water path of marine clouds could be correlated or anticorrelated with

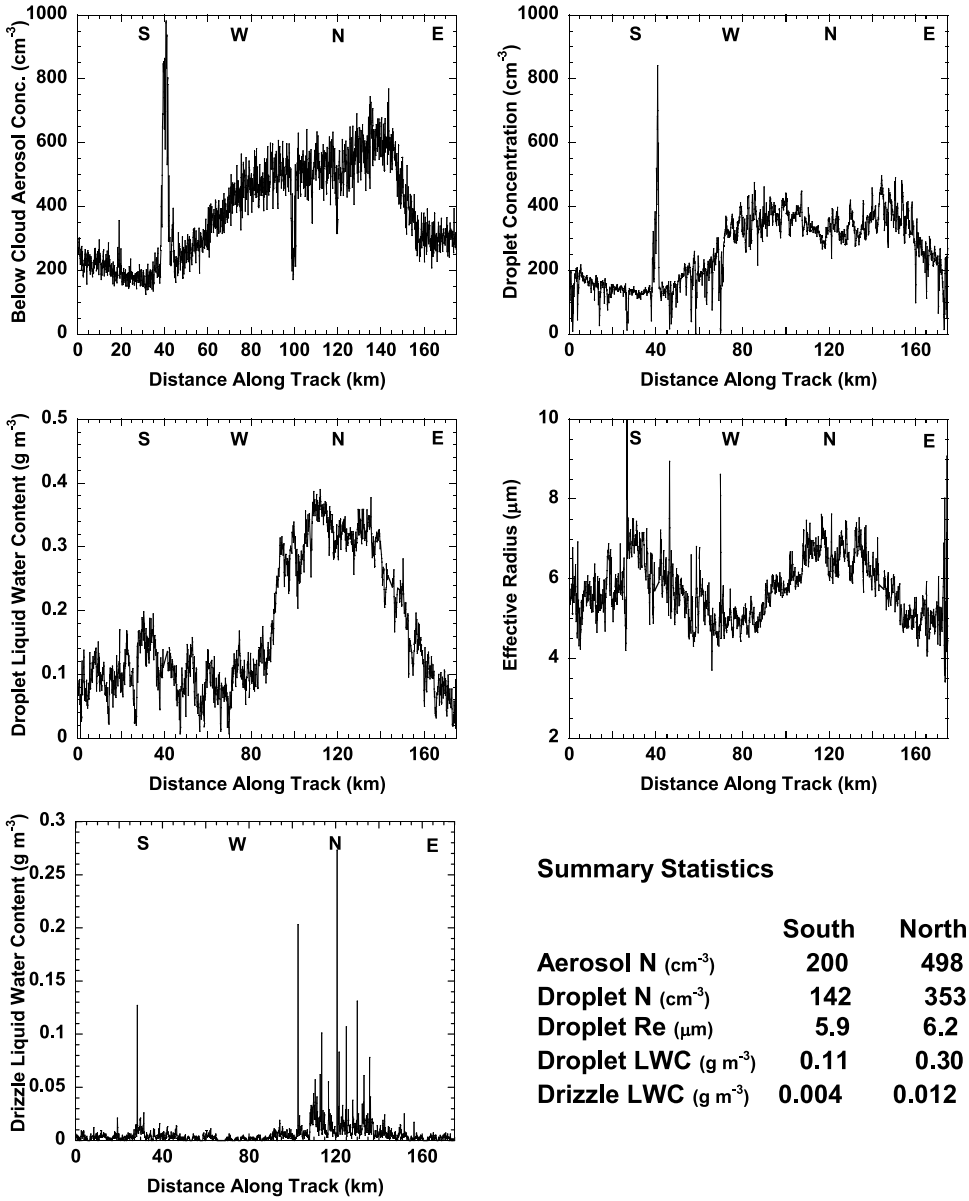

Figure 12. Relationship between aerosol particle concentration and various microphysical properties on flight 3 (nighttime flight). Lower right pane gives mean values for partial legs approximately 36 km long at each side of the track.

aerosol particle concentration, with the anticorrelation occurring primarily in warmer seasons or regions. They hypothesized that in these cases, droplet size, LWC and cloud thickness covaried in response to the dissipative effects of either entrainment or short wave heating. As mentioned above, *Brenguier et al.* [2003] observed that polluted clouds tended to be thinner than clean clouds for the ACE-2 data set over the Atlantic. They suggested another explanation: that polluted clouds, originating in a different air mass, formed in shallower, drier boundary layers.

[46] For DYCOMS-II, total liquid water content was calculated for each flight leg by adding the King hot-wire probe LWC and the 2D-C LWC. In contrast to the hypothesis that clean clouds with large drizzle rates may have lower liquid water contents, no significant correlation between aerosol particle number and LWC is indicated for this data set (t_{obs} = 0.8, t_{crit} = 1.9 for cloud top LWC and t_{obs} = 0.35, t_{crit} = 1.9 for cloud base LWC). Since LWC in stratiform clouds tends to increase with height, some of the variation in LWC might be due to variations in the level of the flight legs flown relative to the height of the cloud (see section 2). Using data from soundings, LWC values were normalized to the project mean flight levels for cloud base and cloud top (0.22 and 0.72, respectively, relative to the actual geometric thickness as described in the next section). This analysis also assumed that LWC increases linearly with height, which is true for the lower 80% of the height of marine stratiform clouds [*Brenguier et al.*, 2003]. These normalized data also showed no significant correlation

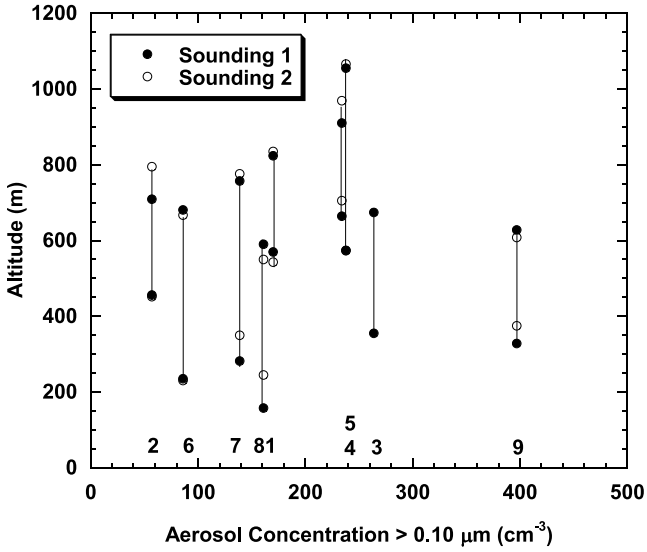

Figure A1. Altitude extent of clouds measured during two different soundings for each flight (except flight 3). Cloud base and cloud top are marked with solid circles for the first sounding, and hollow circles for the second. Altitude derived from the GPS was used.

aerosol particle number and liquid water content. This indicates that other factors are responsible for the large variations (about a factor of two even for similar aerosol concentrations) in LWC from flight to flight. Also of note is that the two cleanest flights (2 and 6) had the largest variability in cloud-top LWC as well as in effective radius throughout the flight legs, in agreement with some modeling studies.

[47] Cloud base height and geometric thickness were calculated following the FSSP frequency distribution technique of *Pawlowska and Brenguier* [2003], except with 1 Hz rather than 10 Hz data. Data from both soundings for each flight are plotted with different symbols in Figure A1. The two daytime flights (8 and 9), where radiative effects may influence cloud thickness [e.g., *Ackerman et al.*, 2003], show some of the greatest variability between individual soundings and had relatively low cloud tops.

[48] Cloud top height and boundary layer thickness appeared to be strongly modulated by the large-scale conditions. During the beginning of the second week of the project (flights 4 and 5), strong cold advection aloft was associated with less large-scale subsidence, a weaker inversion, a deeper boundary layer and more elevated cloud base. Outside of this period, the large-scale conditions were relatively similar, with some tendency toward stronger inversions and greater subsidence toward the end of the project. Despite substantial flight-to-flight variability, three of the four cleanest cloud cases (flights 6, 7, and 8) were relatively thick. Flight 2 does not fit this pattern. This very clean cloud layer was relatively thin and showed large differences between the two soundings. This may have been a case where very low CCN concentrations and drizzle, over time, caused changes in cloud structure and overall thinning [e.g., *Ackerman et al.*, 1993]. Extremely low CCN concentrations are expected to reduce equilibrium cloud-top height and cloud thickness as well as cloud optical depth and liquid water path [*Pincus and Baker*, 1994; *Hegg*, 1999; *Petters*, 2004]. Interestingly, *Brenguier et al.* [2003] also found that their cleanest cloud case, with droplet concentrations of about 50 cm^{-3}, did not fit the overall trend of decreasing thickness with increasing droplet concentration for their data.

[49] Figure A2 shows that cloud geometric thickness is weakly anticorrelated with aerosol particle concentration, if flight 2 is removed from the regression. However, this relationship narrowly passes the significance criterion (t_{obs} = 2.0, t_{crit} = 1.8). It is apparent that variations in geometric thickness are driven primarily by factors other than aerosol particle concentration, such as the large-scale divergence field [e.g., *Schubert*, 1976].

[50] In Figure A3, liquid water path calculated in two different ways is plotted against aerosol particle concentration for the DYCOMS-II data set. In Figure A3a, liquid water path was calculated using the LWC measured during the cloud-top flight leg for each flight, with the additional assumption that liquid water content increased linearly from zero at cloud base to a maximum value at the top of the cloud (cloud-base and cloud-top being determined from the soundings). This yielded a maximum value slightly larger than the cloud-top flight-leg value, which was measured approximately 72% of the distance between cloud base and cloud top. The vertically averaged LWC value for the cloud layer was then multiplied by the cloud geometric thickness (Figure A2) determined from both soundings. In Figure A3b, liquid water path was calculated using actual liquid water data measured by the King hot-wire probe during the individual soundings. (Two hot-wire probes were flown on most flights; while the two gave similar values, the one with an out-of-cloud baseline value closest to zero for the sounding of interest was used here). Using geometric

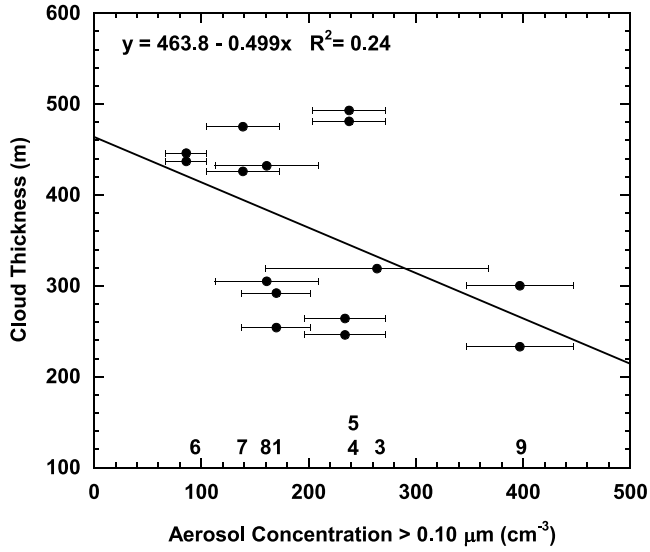

Figure A2. Aerosol particle concentration versus cloud geometric thickness determined from two soundings for each flight (as determined via the *Pawlowska and Brenguier* [2003] method), without the very clean flight 2. Horizontal error bars represent standard deviation as in Figure 1. Note that the curve fit shown here is only valid from about 60 to 400 particles cm^{-3}.

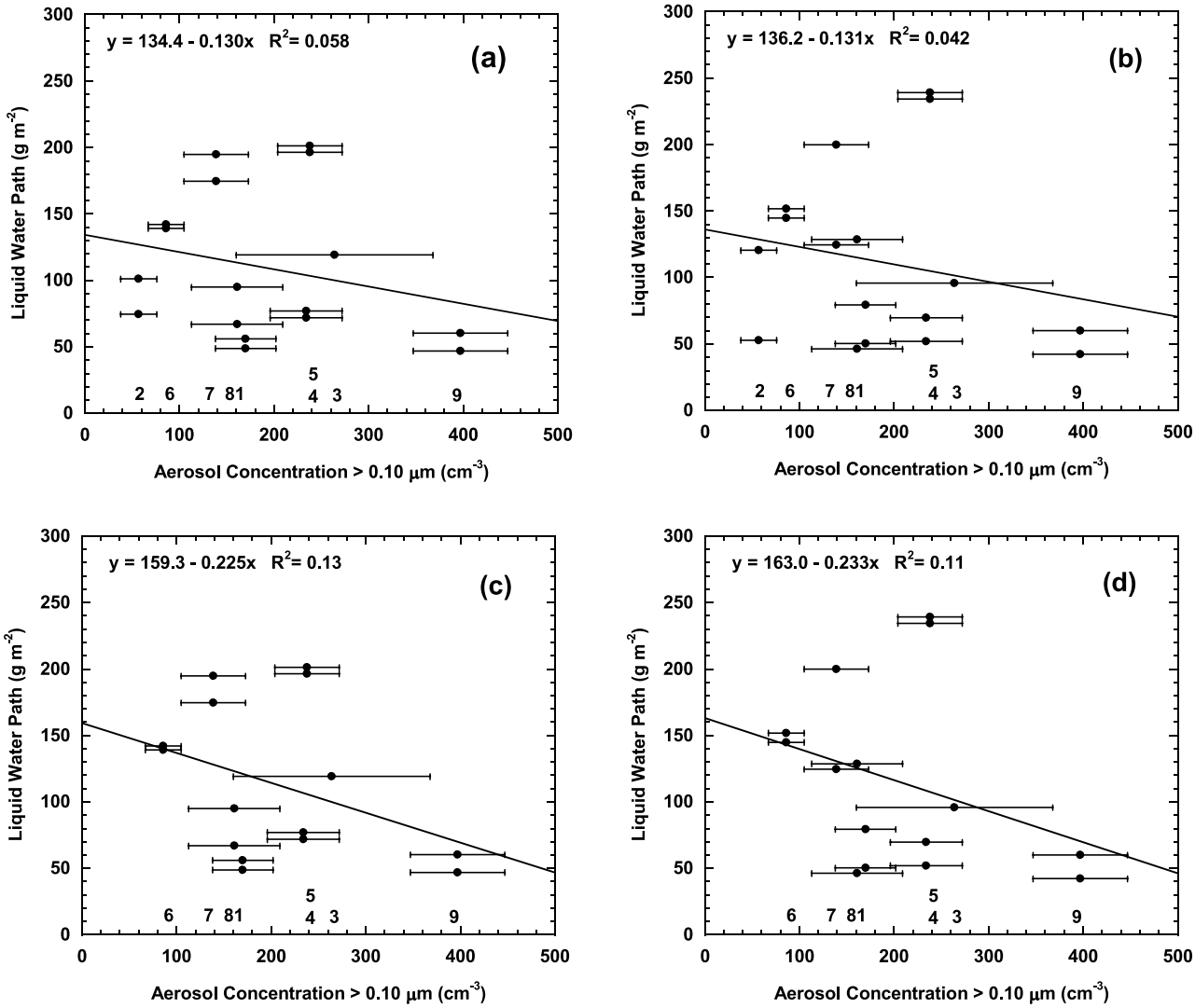

Figure A3. (a) Aerosol particle concentration versus cloud liquid water path. LWP was determined using liquid water content derived from cloud-top average value with the assumption of a linear increase in liquid water content with height above cloud base. Cloud geometric thickness was determined from two soundings for each flight. Horizontal error bars represent standard deviation as in Figure 1. (b) Same as in Figure A3a, but using actual liquid water content measured throughout the soundings to calculate LWP. (c) Same as in Figure A3a, but without the very clean flight 2. (d) Same as in Figure A3b, but without the very clean flight 2. Note that the curve fits shown here are only valid from about 60 to 400 particles cm^{-3}.

thickness from both soundings for each flight gives an indication of the uncertainty due to changes in cloud thickness. Both of the above methods have their own advantages. The first method uses the flight-leg average liquid water content, which represents a larger cloud area, but includes data from only one altitude. Also, it may overestimate LWC due to the neglect of entrainment near cloud top. The second method utilizes actual liquid water content throughout the depth of the cloud, but suffers from a limited spatial sampling area.

[51] Both methods of calculating LWP, however, yield similar results. Magnitudes of liquid water path (as well as those of effective radius, geometric thickness and the optical thickness derived earlier) for the DYCOMS-II data set are similar to those measured in the same region by *Nakajima et al.* [1991]. As in the relationships with geometric thickness, a weak anticorrelation of liquid water path with particle number concentration is observed, but flight-to-flight variations with little relationship to particle number dominate. If the very clean, high-drizzle flight 2 is removed as an outlier (Figures A3c and A3d), the correlation coefficient is slightly higher but the relationship is still not significant (t_{obs} = 1.3, t_{crit} = 1.8).

[52] **Acknowledgments.** This material is based upon work supported by the National Science Foundation under grant 0104707. We also acknowledge the expert assistance of the NCAR crew and technical support staff, including Dave Rogers and Chris Webster for effective radius calculations. James Coakley, Steven Warren, and Jean-Louis Brenguier provided helpful commentary. Jim Anderson and Peter Crozier helped with chemical analyses briefly mentioned here.

References

Ackerman, A. S., O. B. Toon, and P. V. Hobbs (1993), Dissipation of marine stratiform clouds and collapse of the marine boundary layer due to the depletion of cloud condensation nuclei by clouds, *Science*, *262*, 226–228.

Ackerman, A. S., O. B. Toon, D. E. Stevens, A. J. Heymsfield, V. Ramanathan, and E. J. Welton (2000), Reduction of tropical cloudiness by soot, *Science*, *288*, 1042–1047.

Ackerman, A. S., O. B. Toon, D. E. Stevens, and J. A. Coakley Jr. (2003), Enhancement of cloud cover and suppression of nocturnal drizzle in stratocumulus polluted by haze, *Geophys. Res. Lett.*, *30*(7), 1381, doi:10.1029/2002GL016634.

Ackerman, A. S., M. Kilpatrick, D. Stevens, and O. B. Toon (2004), Entrainment, drizzle, and stratocumulus cloud albedo, paper presented at 14th International Conference on Clouds and Precipitation, World Meteorol. Org., Bologna, Italy, 18–23 July.

Albrecht, B. A. (1989), Aerosols, cloud microphysics, and fractional cloudiness, *Science*, *245*, 1227–1230.

Austin, P. H., Y. Wang, R. Pincus, and V. Kujala (1995), Precipitation in stratocumulus clouds: Observational and modeling results, *J. Atmos. Sci.*, *52*, 2329–2352.

Barrett, E. W., F. P. Parungo, and R. F. Pueschel (1979), Cloud modification by urban pollution: A physical demonstration, *Meteorol. Rundsch.*, *32*, 136–149.

Baumgardner, D., W. A. Cooper, and J. E. Dye (1990), Optical and electronic limitations of the forward-scattering spectrometer probe, in *Liquid Particle Size Techniques*, vol. 2, edited by E. D. Hirleman, W. D. Bachalo, and P. G. Felton, *ASTM STP 1083*, pp. 115–127, Am. Soc. for Test. and Mater., West Conshohocken, Pa.

Bougeaut, P. (1985), The diurnal cycle of the marine stratocumulus layer: A higher-order model study, *J. Atmos. Sci.*, *42*, 2826–2843.

Brenguier, J. L., T. Bourrianne, A. A. Coelho, J. Isbert, R. Peytavi, D. Trevarin, and P. Wechsler (1998), Improvements of the droplet size distribution measurements with the Fast-FSSP, *J. Atmos. Oceanic Technol.*, *15*, 1077–1090.

Brenguier, J. L., P. Y. Chuang, Y. Fouquart, D. W. Johnson, F. Parol, H. Pawlowska, J. Pelon, L. Schüller, F. Schröder, and J. R. Snider (2000a), An overview of the ACE-2 CLOUDY- COLUMN Closure Experiment, *Tellus, Ser. B*, *52*, 814–826.

Brenguier, J. L., H. Pawlowska, L. Schuller, R. Preusker, J. Fischer, and Y. Fouquart (2000b), Radiative properties of boundary layer clouds: Droplet effective radius versus number concentration, *J. Atmos. Sci.*, *57*, 803–821.

Brenguier, J. L., H. Pawlowska, and L. Schüller (2003), Cloud microphysical and radiative properties for parameterization and satellite monitoring of the indirect effect of aerosols on climate, *J. Geophys. Res.*, *108*(D15), 8632, doi:10.1029/2002JD002682.

Charlson, R. J., J. E. Lovelock, M. O. Andreae, and S. G. Warren (1987), Oceanic phytoplankton, atmospheric sulphur, cloud albedo and climate, *Nature*, *325*, 655–661.

Charlson, R. J., S. E. Schwartz, J. M. Hales, R. D. Cess, J. A. Coakley Jr., J. E. Hansen, and D. J. Hoffman (1992), Climate forcing by anthropogenic aerosols, *Science*, *255*, 423–430.

Coakley, J. A., and C. D. Walsh (2002), Limits to the aerosol indirect radiative effect derived from observations of ship tracks, *J. Atmos. Sci.*, *59*, 668–680.

Conant, W. C., et al. (2004), Aerosol-cloud drop concentration closure in warm clouds, *J. Geophys. Res.*, *109*, D13204, doi:10.1029/2003JD004324.

Durkee, P. A., K. J. Noone, and R. T. Bluth (2000), The Monterey Area Ship Track experiment, *J. Atmos. Sci.*, *57*, 2523–2541.

Faloona, I., D. Lenschow, T. Campos, B. Stevens, M. Van Zanten, B. Blomquist, D. Thornton, A. Bandy, and H. Gerber (2005), Observations of entrainment in eastern Pacific marine stratocumulus using three conserved scalars, *J. Atmos. Sci.*, in press.

Feingold, G., and P. Y. Chuang (2002), Analysis of the influence of film-forming compounds on droplet growth: Implications for cloud microphysical processes and climate, *J. Atmos. Sci.*, *59*, 2006–2018.

Fitzgerald, J. W., and P. A. Spyers-Duran (1973), Changes in cloud nucleus concentration and cloud droplet size distribution associated with pollution from St. Louis, *J. Appl. Meteorol.*, *12*, 511–516.

Frick, G. M., and W. A. Hoppel (1993), Airship measurements of aerosol size distributions, cloud droplet spectra, and trace gas concentrations in the marine boundary layer, *Bull. Am. Meteorol. Soc.*, *74*, 2195–2202.

Guibert, S., J. R. Snider, and J. L. Brenguier (2003), Aerosol activation in marine stratocumulus clouds: 1. Measurement validation for a closure study, *J. Geophys. Res.*, *108*(D15), 8629, doi:10.1029/2002JD002692.

Gultepe, I., G. A. Isaac, W. R. Leaitch, and C. M. Banic (1996), Parameterizations of marine stratus microphysics based on in situ observations: Implications for GCMS, *J. Clim.*, *9*, 345–357.

Han, Q., W. B. Rossow, and A. A. Lacis (1994), Near-global survey of effective droplet radii in liquid water clouds using ISCCP data, *J. Clim.*, *7*, 465–497.

Han, Q., W. B. Rossow, J. Zeng, and R. Welch (2002), Three different behaviors of liquid water path of water clouds in aerosol-cloud-interactions, *J. Atmos. Sci.*, *59*, 726–735.

Hansen, J. E., and L. D. Travis (1974), Light scattering in planetary atmospheres, *Space Sci. Rev.*, *16*, 527–610.

Hegg, D. A. (1999), Dependence of marine stratocumulus formation on aerosols, *Geophys. Res. Lett.*, *26*, 1429–1432.

Heintzenberg, J., D. C. Covert, and R. Van Dingenen (2000), Size distribution and chemical composition of marine aerosols: A compilation and review, *Tellus, Ser. B*, *52*, 1104–1122.

Hoppel, W. A., G. M. Frick, J. W. Fitzgerald, and R. E. Larson (1994), Marine boundary layer measurements of new particle formation and the effects of nonprecipitating clouds on the aerosol size distribution, *J. Geophys. Res.*, *99*, 14,443–14,459.

Jaffe, D., et al. (1999), Transport of Asian air pollution to North America, *Geophys. Res. Lett.*, *26*, 711–714.

Kim, Y., and R. D. Cess (1993), Effect of anthropogenic sulfate aerosols on low-level cloud albedo over oceans, *J. Geophys. Res.*, *98*, 14,883–14,885.

King, W. D., J. E. Dye, J. W. Strapp, D. Baumgardner, and D. Huffman (1985), Icing wind tunnel tests on the CSIRO liquid water probe, *J. Atmos. Oceanic Technol.*, *2*, 293–303.

Leaitch, W. R., G. A. Isaac, J. W. Strapp, C. M. Banic, and H. A. Wiebe (1992), The relationship between cloud droplet number concentrations and anthropogenic pollution: Observations and climatic implications, *J. Geophys. Res.*, *97*, 2463–2472.

Martin, G. M., D. W. Johnson, and A. Spice (1994), The measurement and parameterization of effective radius of droplets in warm stratocumulus clouds, *J. Atmos. Sci.*, *51*, 1823–1842.

McFarquhar, G. M., and A. J. Heymsfield (2001), Parameterizations of INDOEX microphysical measurements and calculations of cloud susceptibility: Applications for climate studies, *J. Geophys. Res.*, *106*, 28,675–28,698.

Meador, W. E., and W. R. Weaver (1980), Two-stream approximations to radiative transfer in planetary atmospheres: A unified description of existing methods and a new improvement, *J. Atmos. Sci.*, *37*, 630–643.

Nakajima, T., M. D. King, J. D. Spinhirne, and L. F. Radke (1991), Determination of the optical thickness and effective particle radius of clouds from reflected solar radiation measurements. Part II: Marine stratocumulus observations, *J. Atmos. Sci.*, *48*, 728–750.

Nakajima, T., A. Higurashi, K. Kawamoto, and J. E. Penner (2001), A possible correlation between satellite-derived cloud and aerosol microphysical properties, *Geophys. Res. Lett.*, *28*, 1171–1174.

Noonkester, V. R. (1984), Droplet spectra observed in marine stratus cloud layers, *J. Atmos. Sci.*, *41*, 829.

O'Dowd, C. D., J. Lowe, M. H. Smith, and A. D. Kaye (1999), The relative importance of sea-salt and nss-sulphate aerosol to the marine CCN population: An improved multi-component aerosol-droplet parameterization, *Q. J. R. Meteorol. Soc.*, *125*, 1295–1313.

Pawlowska, H., and J.-L. Brenguier (2003), An observational study of drizzle formation in stratocumulus clouds for general circulation model (GCM) parameterizations, *J. Geophys. Res.*, *108*(D15), 8630, doi:10.1029/2002JD002679.

Petters, M. D. (2004), Cloud condensation nuclei: Measurement, prediction and effects on remote marine stratocumulus clouds, Ph.D. dissertation, 154 pp., Univ. of Wyoming, Laramie.

Pincus, R., and M. B. Baker (1994), Effect of precipitation on the albedo susceptibility of clouds in the marine boundary layer, *Nature*, *372*, 250–252.

Platnick, S., and S. Twomey (1994), Determining the susceptibility of cloud albedo to changes in droplet concentration with the Advanced Very High Resolution Radiometer, *J. Appl. Meteorol.*, *33*, 334–347.

Radke, L. F., J. A. Coakley Jr., and M. D. King (1989), Direct and remote sensing observations of the effects of ships on clouds, *Science*, *246*, 1146–1148.

Raga, G. B., and P. R. Jonas (1993), On the link between cloud-top radiative properties and sub-cloud aerosol concentrations, *Q. J. R. Meteorol. Soc.*, *119*, 1419–1425.

Rosenfeld, D. (2000), Suppression of rain and snow by urban and industrial air pollution, *Science*, *287*, 1793–1796.

Russell, L. M., S. H. Zhang, R. C. Flagan, J. H. Seinfeld, M. R. Stolzenburg, and R. Caldow (1996), Radially classified aerosol detector for aircraft-based submicron aerosol measurements, *J. Atmos. Oceanic Technol.*, *13*, 598–609.

Sassen, K., D. Starr, G. G. Mace, M. R. Poellot, S. H. Melfi, W. L. Eberhard, J. D. Spinhirne, E. W. Eloranta, D. E. Hagan, and J. Hallett (1995), The 5–6 December 1991 FIRE IFO-II jet-stream cirrus case-study—Possible influences of volcanic aerosols, *J. Atmos. Sci.*, *52*, 97–123.

Schubert, W. H. (1976), Experiments with Lilly's cloud-topped mixed layer model, *J. Atmos. Sci.*, *33*, 436–446.

Schüller, L., J. L. Brenguier, and H. Pawlowska (2003), Retrieval of microphysical, geometrical, and radiative properties of marine stratocumulus from remote sensing, *J. Geophys. Res.*, *108*(D15), 8631, doi:10.1029/2002JD002680.

Snider, J. R., S. Guibert, J.-L. Brenguier, and J.-P. Putand (2003), Aerosol activation in marine stratocumulus clouds: 2. Köhler and parcel theory closure studies, *J. Geophys. Res.*, *108*(D15), 8629, doi:10.1029/2002JD002692.

Stephens, G. L. (1978), Radiation profiles in extended water clouds, II, Parametrization schemes, *J. Atmos. Sci.*, *35*, 2123–2132.

Stevens, B., W. R. Cotton, G. Feingold, and C. H. Moeng (1998), Large eddy simulations of strongly precipitating, shallow, stratocumulus-topped boundary layers, *J. Atmos. Sci.*, *55*, 3616–3638.

Stevens, B., et al. (2003), Dynamics and chemistry of marine stratocumulus—DYCOMS-II (and electronic supplement), *Bull. Am. Meteorol. Soc.*, *84*, 579–593.

Stevens, B., G. Vali, K. Comstock, R. Wood, M. C. Van Zanten, P. H. Austin, C. S. Bretherton, and D. H. Lenschow (2005), Pockets of open cells (POCs) and drizzle in marine stratocumulus, *Bull. Am. Meteorol. Soc.*, *86*(1), 51–57, doi:10.1175/BAMS-86-1-51.

Ström, J., and S. Ohlsson (1998), In situ measurements of enhanced crystal number densities in cirrus clouds caused by aircraft exhaust, *J. Geophys. Res.*, *103*, 11,355–11,361.

Taylor, J. P., M. D. Glew, J. A. Coakley Jr., W. R. Tahnk, S. Platnick, P. V. Hobbs, and R. J. Ferek (2000), Effects of aerosols on the radiative properties of clouds, *J. Atmos. Sci.*, *57*, 2656–2670.

Twohy, C. H. (1991), Airborne Condensation Nucleus Counter user's guide, *Tech. Note TN-356+EDD*, 21 pp., Natl. Cent. for Atmos. Res., Boulder, Colo.

Twohy, C. H., A. D. Clarke, S. G. Warren, L. F. Radke, and R. J. Charlson (1989), Light-absorbing material extracted from cloud droplets and its effect on cloud albedo, *J. Geophys. Res.*, *94*, 8623–8631.

Twohy, C. H., P. A. Durkee, B. J. Huebert, and R. J. Charlson (1995), Effects of aerosol particles on the microphysics of coastal stratiform clouds, *J. Clim.*, *8*, 773–783.

Twohy, C. H., J. G. Hudson, S. S. Yum, J. R. Anderson, S. K. Durlak, and D. Baumgardner (2001), Characteristics of cloud nucleating aerosols in the Indian Ocean region, *J. Geophys. Res.*, *106*, 28,699–28,710.

Twomey, S. (1974), Pollution and the planetary albedo, *Atmos. Environ.*, *8*, 1251–1256.

Twomey, S. (1991), Aerosols, clouds and radiation, *Atmos. Environ., Part A*, *25*, 2435–2442.

VanReken, T. M., T. A. Rissman, G. C. Roberts, V. Varutbangkul, H. H. Jonsson, R. C. Flagan, and J. H. Seinfeld (2003), Toward aerosol/cloud condensation nuclei (CCN) closure during CRYSTAL-FACE, *J. Geophys. Res.*, *108*(D20), 4633, doi:10.1029/2003JD003582.

Van Zanten, M. C., B. Stevens, G. Vali, and D. H. Lenschow (2005), Observations of drizzle in nocturnal marine stratocumulus, *J. Atmos. Sci.*, in press.

Vong, R. J., and D. S. Covert (1998), Simultaneous observations of aerosol and cloud droplet size spectra in marine stratocumulus, *J. Atmos. Sci.*, *55*, 2180–2192.

Weber, R. J., A. D. Clarke, M. Litchy, J. Li, G. Kok, R. D. Schillawski, and P. H. McMurry (1998), Spurious aerosol measurements when sampling from aircraft in the vicinity of clouds, *J. Geophys. Res.*, *103*, 28,337–28,346.

Wetzel, M. A., and L. L. Stowe (1999), Satellite-observed patterns in stratus microphysics, aerosol optical thickness, and shortwave radiative forcing, *J. Geophys. Res.*, *104*, 31,287–31,299.

Yum, S. S., and J. G. Hudson (2002), Maritime/continental microphysical contrasts in stratus, *Tellus, Ser. B*, *54*, 61–73.

F. Burnet, Meteo-France, Centre National de Recherches Météorologiques, Météorologie Expérimentale et Instrumentale, MNP, 31057 Toulouse, France. (burnet@cnrm.meteo.fr)

M. D. Petters and J. R. Snider, Department of Atmospheric Sciences, University of Wyoming, Laramie, WY 82701, USA. (petters@uwyo.edu; jsnider@uwyo.edu)

L. Russell, Scripps Institution of Oceanography, University of California, San Diego, La Jolla, CA 92093-0221, USA. (lmrussell@ucsd.edu)

B. Stevens, Department of Atmospheric Sciences, University of California, Los Angeles, CA 90095-1565, USA. (bstevens@atmos.ucla.edu)

W. Tahnk and C. H. Twohy, College of Oceanic and Atmospheric Sciences, Oregon State University, Corvallis, OR 97331-5503, USA. (tahnk@oce.orst.edu; twohy@oce.orst.edu)

M. Wetzel, Desert Research Institute, Reno, NV 89512, USA. (melanie.wetzel@dri.edu)